

621-762 : 539.383 : 621-288

An Investigation of Air-leakage between Contact Surfaces*

(2nd Report, On Case in which the Deformation of Surface Irregularities was Assumed to be Elasto-plastic)

By Tsuneji KAZAMAKI**

In the case in which a specimen was pressed against a rigid smooth surface, assuming its surface irregularities had a form of similar truncated cone in the same manner as the 1st report and the deformation of the truncated cone was elasto-plastic, the analytical values of equivalent gap for the fluid leakage between them were derived considering the permanent reduction of the central height of surface roughness. The results obtained can be summarized as follows :

(1) The analytical values of equivalent gap obtained by assuming the surface irregularities as elasto-plastic were in agreement with the experimental values with a deviation of about 7%, excepting the condition of which the applied load was low, i. e. less than about 5kg/cm², where abnormally high surface irregularities existed on the surface roughness. The values obtained by assuming the surface irregularities as ideally plastic, furthermore, were derived in the same results as above.

(2) The analytical expression of balance conditions between applied load and supplied gas pressure between contact surfaces was derived and the analytical values were in good agreement with the experimental results.

1. Introduction

In the 1st report⁽¹⁾, the analytical values of equivalent gap for the fluid leakage between contact surfaces were derived for a case in which a specimen was pressed against a rigid smooth surface, assuming its surface irregularities had a form of similar truncated cone and were ideally elastic or plastic, and the conclusions were derived as follows : the values of equivalent gap obtained by assuming the surface irregularities as ideally plastic were in agreement with the experimental values with a deviation within about 7%.

In this paper, the deformation of surface irregularities was assumed to be elasto-plastic and the analytical expressions for the equivalent gap between contact surfaces were derived, where the permanent reduction of the central height of surface irregularities, which varies depending on the applied load, was determined by experiments, and the conical angle of the truncated cones and the s -values decided by the profiles of surface ir-

regularities were considered.

The analytical expression of balance conditions, furthermore, between applied load and supplied gas pressure between contact surface was derived.

2. Nomenclature

- $H_{\max 0}$: maximum height of various surface irregularities without applied load
- h_{c0} : central height of surface irregularities without applied load
- h_c : ditto (with applied load)
- p_c : applied load per unit area on contact surface
- p_{1c} : increased applied load per unit area on contact surface
- δ : displacement depending on the elasto-plastic deformation of surface irregularities
- θ : permanent reduction of the central height of surface roughness
- $\Theta_{(\beta)}, K_{(\beta)}, G_{(\beta)}$: functions of β
- $f_{(s)}$: function of s
- R_e : Reynolds number
- $\eta = (h_{c0}/H_{\max 0})_{\text{mean}}$
- mean : arithmetic mean

* Received 7th January, 1970.

** Assistant Professor, Faculty of Engineering, Toyama University, Takaoka.

3. Theoretical analysis

Assuming that the displacement of surface irregularities depending on applied load is the sum of ξ_{el} and ξ_{pl} , which represent the respective displacements depending on the elastic and the plastic deformations for various truncated cones, we have

$$\left. \begin{aligned} \delta &= \xi_{el} + \xi_{pl} \\ &= P_m \{ (\sqrt{s}-1)^2 / \sqrt{s} \} / EH\pi \tan^2 \gamma \\ &\quad + \sqrt{P_m / \pi k \sigma_s} / \tan \gamma \equiv H - Z_0 \end{aligned} \right\} \dots\dots\dots(1)$$

where we put

$$\left. \begin{aligned} (\sqrt{s}-1)^2 / \sqrt{s} E \pi \tan^2 \gamma &= X \\ 1 / \sqrt{\pi k \sigma_s} \tan \gamma &= Y \end{aligned} \right\} \dots\dots\dots(2)$$

and then Eq. (1) will be described by

$$H - Z_0 = P_m(X/H) + \sqrt{P_m} Y \dots\dots\dots(1)'$$

and then the applied load on any truncated cone is given by

$$P_m = \frac{[2(H - Z_0)(X/H) + Y^2 \pm Y^2 \times \sqrt{1 + 4(H - Z_0)(X/HY^2)}]}{2(X/H)^2} \dots\dots\dots(3)$$

The applied load, accordingly, on any truncated cone requires two different values as follows :

$$\begin{aligned} P_m &= 2(H - Z_0)(H/X) + (Y/X)^2 H^2 - (H - Z_0)^2 / Y^2 + 2(H - Z_0)^3 (X/HY^4) \dots\dots\dots(4 \cdot a) \\ &= \{ (H - Z_0)/Y \}^2 - 2(H - Z_0)^3 (X/HY^4) \dots\dots\dots(4 \cdot b) \end{aligned}$$

and here, only Eq. (4.b) might be applied for the applied load on any truncated cone. (The details of the calculation are shown in the Appendix).

Now we put

$$X/Y^2 = Z \dots\dots\dots(5)$$

and then the applied load on any truncated cone becomes

$$P_m = \{ (H - Z_0)^2 - 2Z(H - Z_0)^3/H \} / Y^2 \dots\dots\dots(4 \cdot b)'$$

Thus the total applied load on a nominal area will be described by

$$\begin{aligned} P_c &= N \int_{Z_0}^{\infty} P_m f_{(H)} dH \\ &= NC \frac{3\sqrt{\pi}}{8} \frac{\alpha^5}{Y^2} \left[1 + \frac{2}{3} \beta^2 - \frac{2}{3\sqrt{\pi}} \beta e^{-\beta^2} \right] \\ &\quad - \left(1 + \frac{2}{3} \beta^2 \right) \frac{2}{\sqrt{\pi}} \int_0^{\beta} e^{-\lambda^2} d\lambda - 2Z \end{aligned}$$

Table 3 $I_{(\beta)} = \left\{ \frac{k\sigma_s}{E} \cdot \frac{(\sqrt{s}-1)^2}{\sqrt{s}} \right\}^{-a} \times e^{-b\beta^2}$ Specimen S45C

β	a			b		
	0.890	0.873	0.802	0.880	0.860	0.768
	1.373	1.372	1.362	1.373	1.372	1.362
0.2	195.501	90.013	15.892	124.613	57.428	10.029
0.4	165.803	76.348	13.496	105.683	48.710	8.517
0.6	125.990	58.027	10.278	80.307	37.021	6.486
0.8	85.779	39.518	7.019	54.676	25.212	4.430
1.0	52.324	24.115	4.299	33.352	15.385	2.713
1.2	28.599	13.186	2.361	18.229	8.413	1.490
1.4	14.005	6.461	1.163	8.927	4.122	0.734
1.6	6.145	2.836	0.514	3.917	1.810	0.324
1.8	2.416	1.116	0.203	1.540	0.712	0.128
2.0	0.851	0.393	0.072	0.542	0.251	0.046
s	5	10	10 ²	5	10	10 ²

(For $0.6 \leq \beta \leq 1.4$; error $\leq 6\%$)

Table 2 $\theta_{(\beta)} = \{ \Psi_{(\beta)}/x \} - K_{(\beta)}$ Specimen S45C

Mechanical properties	Annealed $\left\{ \begin{array}{l} E=2.1 \times 10^4 \text{ kg/mm} \\ \sigma_s=35 \text{ kg/mm}^2 \text{ (Lower limit)} \\ k=2.2 \text{ (Lower limit)} \end{array} \right.$			Hardened $\left\{ \begin{array}{l} E=2.1 \times 10^4 \text{ kg/mm}^2 \\ \sigma_s=50 \text{ kg/mm}^2 \text{ (Lower limit)} \\ k=2.4 \text{ (Lower limit)} \end{array} \right.$			
	s	5	10	10 ²	5	10	10 ²
β							
0.2		288.413	132.618	23.189	184.619	84.651	14.433
0.4		200.588	92.303	16.243	128.446	58.962	10.158
0.6		132.816	61.155	10.821	85.074	39.091	6.794
0.8		83.317	38.384	6.823	53.381	24.549	4.298
1.0		49.301	22.723	4.055	31.594	14.540	2.561
1.2		27.407	12.636	2.262	17.566	8.089	1.432
1.4		14.265	6.579	1.181	9.144	4.213	0.749
1.6		6.975	3.218	0.579	4.472	2.061	0.368
1.8		3.189	1.472	0.265	2.045	0.943	0.169
2.0		1.356	0.626	0.113	0.869	0.401	0.072

$$\begin{aligned} & \times \left\{ \left(1 + \frac{2}{3\sqrt{\pi}} \beta e^{-\beta^2} - \frac{2}{\sqrt{\pi}} \int_0^\beta e^{-\lambda^2} d\lambda \right) + 2\beta^2 - \frac{8}{3\sqrt{\pi}} \beta e^{-\beta^2} - 2\beta^2 \frac{2}{\sqrt{\pi}} \int_0^\beta e^{-\lambda^2} d\lambda \right\} \\ & = NC \frac{3\sqrt{\pi}}{8} \frac{\alpha^5}{Y^2} \left[\Psi_{(\beta)} - \chi \{ 2\Phi_{(\beta)} - 4\beta^2 \left(\frac{4}{3\sqrt{\pi}} \frac{e^{-\beta^2}}{\beta} + \frac{2}{\sqrt{\pi}} \int_0^\beta e^{-\lambda^2} d\lambda - 1 \right) \} \right] \\ & = NC (3\sqrt{\pi}/8) \alpha^5 (\chi/Y^2) \Theta_{(\beta)} \dots\dots\dots (6) \end{aligned}$$

where, $\Theta_{(\beta)} = \left\{ \begin{aligned} & \Psi_{(\beta)}/\chi - K_{(\beta)} \\ & K_{(\beta)} = 2\Phi_{(\beta)} - 4\beta^2 G_{(\beta)} \\ & G_{(\beta)} = \frac{4}{3\sqrt{\pi}} \frac{e^{-\beta^2}}{\beta} + \frac{2}{\sqrt{\pi}} \int_0^\beta e^{-\lambda^2} d\lambda - 1 \end{aligned} \right\} \dots\dots\dots (7)$

Here, $K_{(\beta)}$, $G_{(\beta)}$ and $\Theta_{(\beta)}$ which may differ with the material are listed in Tables 1 and 2, respectively, for varying values of β .

Then, introducing Eqs. (2), (5) and the values of N and C given by the 1st report into Eq. (6), the total applied load will be described by

$$P_c = ((\sqrt{s}-1)^4/s\sqrt{s}) (k^2\sigma_s^2/E) S_n \varphi_{(s)} \Theta_{(\beta)} \dots\dots\dots (6)'$$

As the result in the case in which $\Theta_{(\beta)}$ may be replaced by $I_{(\beta)}$ as follows :

$$\Theta_{(\beta)} \doteq I_{(\beta)} = \left\{ \frac{k\sigma_s}{E} \frac{(\sqrt{s}-1)^2}{\sqrt{s}} \right\}^{-a} e^{-b\beta^2} \dots\dots\dots (8)$$

The total applied load may be derived by

$$P_c \doteq 1.117 \left(\frac{\sqrt{s}-1}{\sqrt{s}} \right)^2 k\sigma_s \left\{ \frac{k\sigma_s}{E} \frac{(\sqrt{s}-1)^2}{\sqrt{s}} \right\}^{1-a} S_n \exp\{-(0.72+b)\beta^2\} \dots\dots\dots (9)$$

The height from the base plane of surface roughness, accordingly, will be described by

$$Z_0 = \frac{\alpha}{\sqrt{0.72+b}} \sqrt{\ln \left[1.117 \left(\frac{\sqrt{s}-1}{\sqrt{s}} \right)^2 \frac{k\sigma_s}{p_c} \left\{ \frac{k\sigma_s}{E} \frac{(\sqrt{s}-1)^2}{\sqrt{s}} \right\}^{1-a} \right]} \dots\dots\dots (10)$$

In the case in which the deformation of surface irregularities is assumed to be elasto-plastic, consequently, the equivalent gap will be derived as

$$\frac{H_{ep}}{h_c} = 1.994 f_{(s)} \sqrt{\ln \left[1.117 \left(\frac{\sqrt{s}-1}{\sqrt{s}} \right)^2 \frac{k\sigma_s}{p_c} \left\{ \frac{k\sigma_s}{E} \frac{(\sqrt{s}-1)^2}{\sqrt{s}} \right\}^{1-a} \right]} - 1 \dots\dots\dots (11)$$

where, $f_{(s)} = \zeta/\sqrt{0.72+b} \dots\dots\dots (12)$

The values of $I_{(\beta)}$ are listed in Table 2 for varying values of β and parameters a , b and $f_{(s)}$ are shown in Figs. 1, 2 and 3, respectively, for carbon steel of S45C, and furthermore, the characteristic curves represented by Eq. (11) are shown in Fig. 4.

4. Experiments

4.1 Experimental procedure

The process of measurement is shown in Fig. 5 and the arrangement of the parts to avoid moisture and dust in the air flow, the control of variation of air pressure during the measurement and the method

Table 4 Mechanical properties of experimental materials

Materials		Mechanical properties			Heat treatment	Finishing; lapping	
Symbols	Notations	E kg/mm ²	σ_s kg/mm ²	Hardness H_R			
Specimens	A	S45C	2.1×10 ⁴	35	B 82	550~570°C, 1.5hr heating, furnace cooling	No. 80 of carborundum powder
	B	S45C	2.1	50	C 56	830°C, 1.5hr heating, water cooling	ditto
	C	S45C	2.1	35	B 91	ditto with A	No. 120 of carborundum powder
	D	S45C	2.1	50	C 55	ditto with B	ditto
Base plate		SKS2	2.1	~	C 60	850°C, 1hr heating, oil quench, 180°C, 1hr heating, tempering	Chrome oxide

σ_s : Yield point, lower limit
 H_R : Rockwell hardness
 B, C: Class of Rockwell hardness

of the measurement of air-leakage are similar to the 1st report, but the base plate holder is clamped with the specimen holder by bolts.

It may be supposed that the reduction of applied load, therefore, depending on the fluctuation of the situation clamped by bolts, occurs to the apparatus, and then a similar clamping force for every one of the bolts, i. e. 15~18kg/mm², was control-

ed through the experiments by the observation of the variation of the elongation of the bolts with strain gauges. As the result above-mentioned, the elongation of the bolts was not observed by strain meter when the inlet air pressure of 10 kg/cm² g was applied over the base plate and the displacement of feeling pin attached on the lower part of the base plate was 2 or 3 microns.

Table 5 Numerical values of surface roughness; without applied load (μ)

Direction of tracing		Central height h_{c0}						Maximum height H_{max0}						
		a	b	c	l	m	n	h_{c0mean}	a	b	c	l	m	n
Materials	A	13.63	15.41	13.29	15.60	13.75	15.89	14.60	28.8 (24.2)	34.3 (20.5)	27.0 (25.5)	37.0 (23.0)	29.0 (22.0)	34.0 (22.4)
	B	11.97	12.53	13.74	15.72	15.20	12.49	13.61	25.4 (21.0)	24.5 (21.5)	25.0 (23.8)	38.0 (19.6)	35.0 (17.0)	30.0 (21.0)
	C	8.44	9.37	10.40	10.30	10.40	9.53	9.74	16.5 (14.8)	18.5 (14.5)	16.5 (13.0)	22.3 (15.5)	19.5 (16.5)	18.5 (14.5)
	D	7.70	9.74	5.22	7.65	8.14	7.90	7.73	14.1 (10.0)	21.5 (10.0)	12.0 (8.2)	21.0 (10.8)	18.5 (11.8)	17.0 (11.5)
Base plate		$h_c \sim H_{max} < 0.3$						Note: (1) Methods of measurement are shown in the 1st report (2) The values in brackets are obtained by using the base plane length prescribed by Japan Industrial Standards						

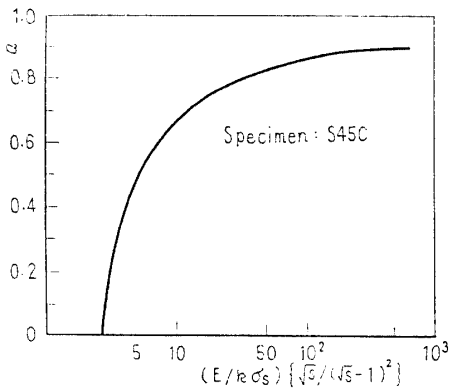


Fig. 1 Variation of a with mechanical properties and s -values of specimen: the figure enables both of annealed steel and hardened steel to be used in common

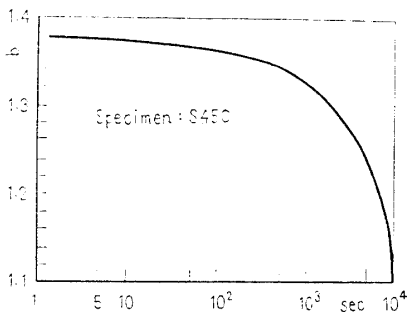


Fig. 2 s -values vs b : the figure enables both of annealed steel and hardened steel to be used in common

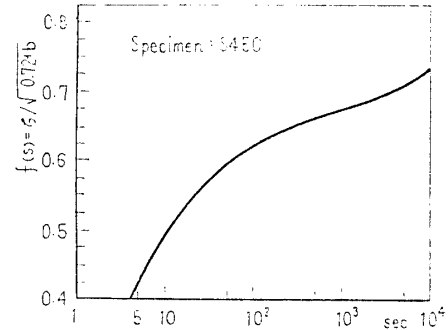


Fig. 3 s -values vs $f(s)$: the figure enables both of annealed steel and hardened steel to be used in common

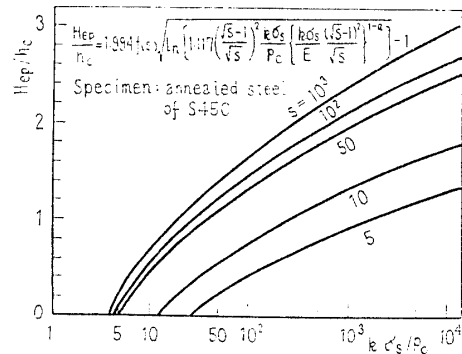


Fig. 4 Characteristic curves: assumed that the truncated cone is elasto-plastic

4.2 Specimens

The form of specimens was equal to the 1st report and the mechanical properties of experimental materials are listed in Table 4 and the profiles of surface roughness, the numerical values, respectively, are shown in Figs. 6, 7 and Table 5.

4.3 Experimental results

4.3.1 Values of γ and s :

The results obtained for them are shown in Figs. 9 and 10. Here, the surface roughness was magnified as shown in Fig. 8 by using a magnifying apparatus of surface roughness produced by authors. The apparatus can be magnified on the same scale for ordinate and abscissa of the profiles of surface roughness; the errors were 2~5mm per 5 meters in the transverse direction, 1~3mm per 550mm in the vertical direction and about 1/4-degree for the rate of perpendicular.

4.3.2 Air-leakage

The experimental results are shown in Fig.

11, for example, they were obtained in eight steps from 1.12 to 30.7kg/cm² for the applied load by spring force, and further are shown in Fig. 12 in three steps, i. e. 1.62, 5.64 and 10.6 kg/cm² for the applied load, after the increased applied loads of six steps from 5.40x10 to 3.24 x10³kg/cm² were applied in order of magnitude by a universal testing machine.

5. Considerations

5.1 Values of γ and s

The distributions over some extent due to the statistical characteristics of γ and s , which shall be considered as influenced by material and the grade of surface finishing as shown in Figs. 9 and 10, may be permitted to these values.

γ -values: the frequency of γ -values is inclined to a large degree to depend on applied load, for example, as shown in an increased applied load, i. e. $p_{10} \approx 11$ kg/mm² (material, D), but no distinct difference is recognized. According to the results

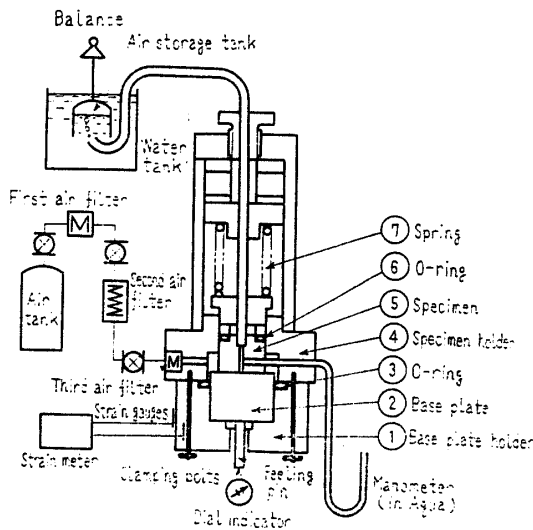
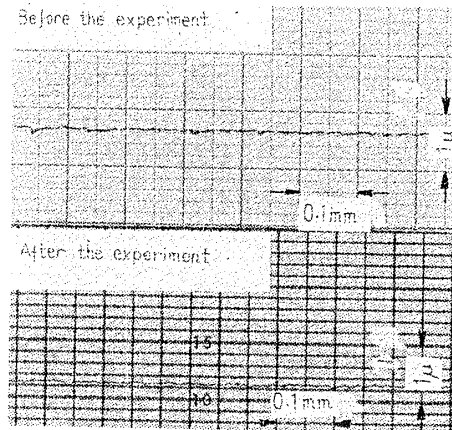
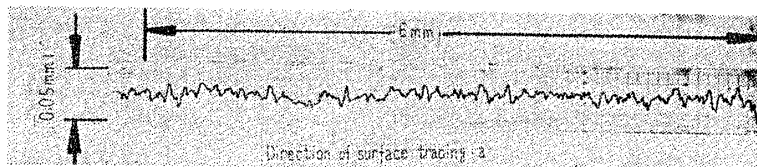


Fig. 5 Process of measurement

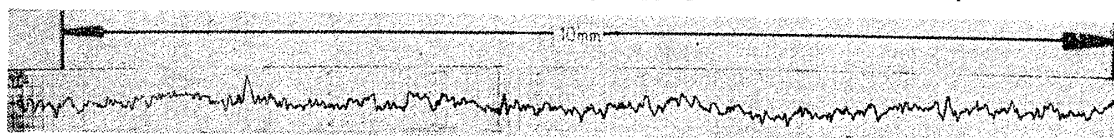


Magnification Ordinate $\times 10\,000 \times 2/3$
Abscissa $\times 100 \times 2/3$

Fig. 6 Profiles of surface roughness of base plate



Specimen: Hardened steel of S45C, Finishing: Lapping, No. 80 of carborundum powder



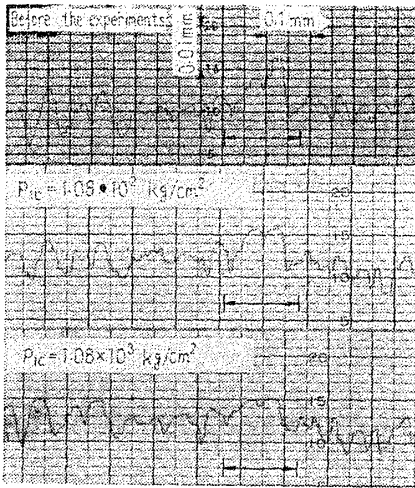
Direction of surface tracing: l Magnification Ordinate $\times 1\,000 \times 3/7$
Abscissa $\times 100 \times 3/7$

Fig. 7 Profiles of surface roughness of specimen (before the experiments): the meaning of the direction of surface tracing, a and l are shown in the 1st report

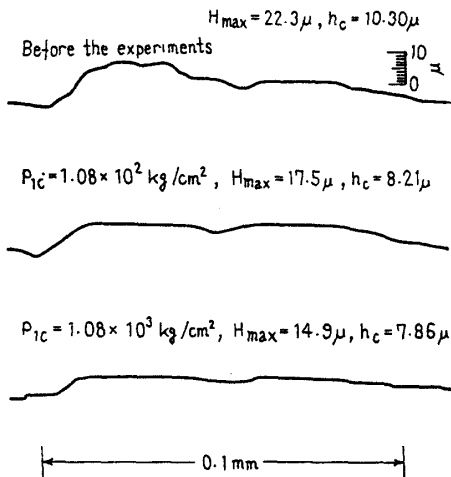
described above, it seems to be quite all right to consider that the γ -values for specimens are independent of the applied load. The values of γ and k as listed in Table 6, accordingly, will be taken for the experiments.

s-values : the distributions without applied load are $s=6\sim 18$ and $4\sim 18$, respectively, for No. 80 and No. 120 of carborundum powder, and then the difference depending on the number of carborundum powder may be recognized more or less in the frequency for the *s*-values.

It may be considered that the distributions of the *s*-values were divided into two main groups which included $s=4\sim 10$ and $10\sim 18$, and this may



(a) Profiles of surface roughness



(b) Profiles of surface roughness magnified on same scale for ordinate and abscissa: (1) the profiles between two arrows in Fig. (a) are magnified (2) the figures are reversed in the directions of tracing compared with Fig. (a) due to magnifying apparatus

Fig. 8 Variation of surface roughness depending on applied load (material: C)

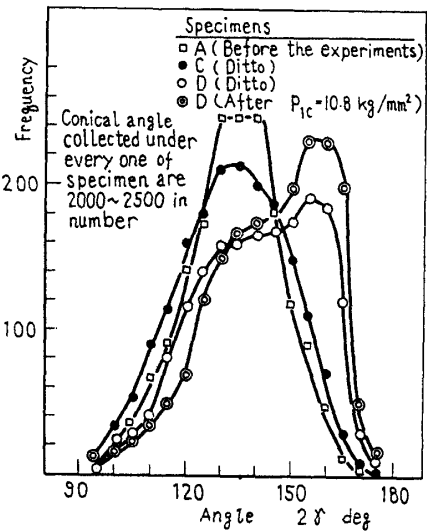


Fig. 9 Distribution of conical angle of surface irregularities

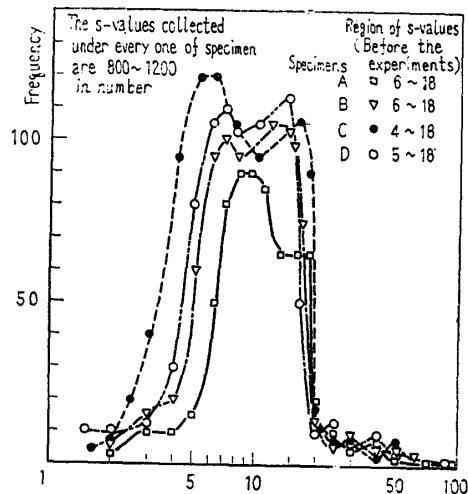


Fig. 10 Distribution of *s*-values: before the experiments

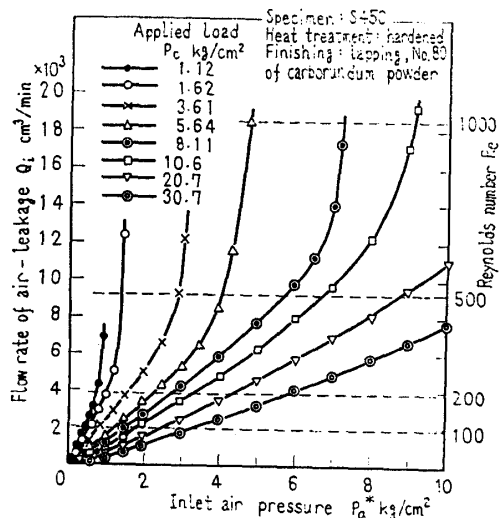
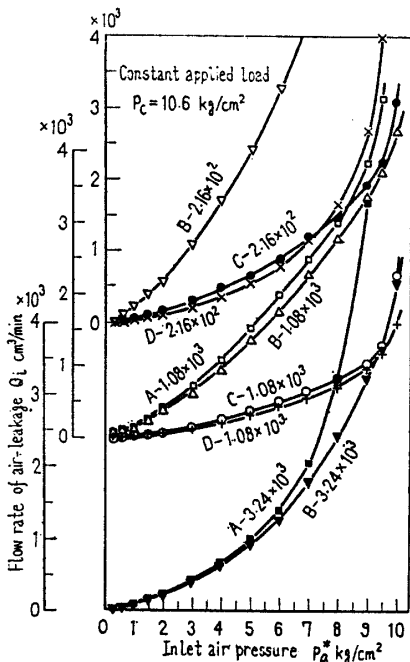
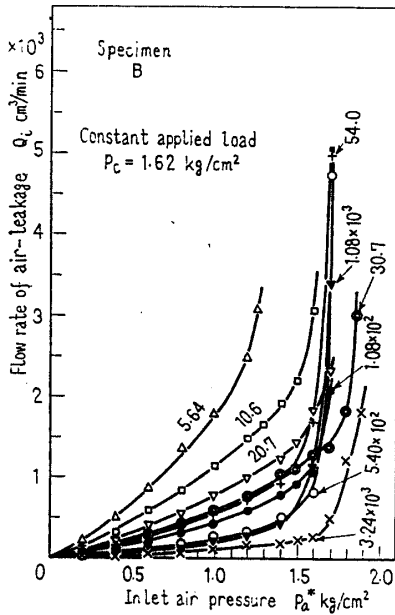


Fig. 11 Experimental results

Table 6 Values of γ and k

Specimens		2γ deg		k Lower limit
Symbols	Heat treatment	Region mean		
A, C	Annealed	130~140	133	2.2
B, D	Hardened	150~160	155	2.4



Note: (1) The meaning of symbols of A, B, C and D is shown in Table 4
 (2) The numerical values are the applied loads in kg/cm²

Fig. 12 Experimental results with constant applied loads after the increased applied loads were applied in order of magnitude

be influenced by the poor uniformity of carborundum powder and the degree of lapping technique.

As described above, the s -values without applied load will be taken as $s=15$ and 12 , respectively, for No. 80 and No. 120 of carborundum powder. Next, the characteristics depending on applied load per unit area are shown in Fig. 13 and it may be said as follows; the s -values in the group of $s=10\sim18$ diminish gradually and those in the other group, i. e. $s=4\sim10$, do not vary.

It seems that the s -values may be distributed over $4\sim10$, consequently, after the applied load exceeds about 200kg/cm^2 .

Neglecting the effect of the recovery of surface irregularities, however, the consideration above-mentioned is based on the numerical values of the surface roughness after an applied load was removed, and then the s -values of which applied loads are kept are doubtful.

5.2 Variation of surface roughness depending on applied load

It seems difficult to record the surface roughness exactly at the same place with and without an applied load, and yet author's every efforts were rendered to do so, for example, as shown in Fig. 8.

5.2.1 Phenomenon of surface irregularities being broken down

The phenomenon that one part of the irregularities on the real contact surface of rough surface, of the specimen which was pressed against a rigid smooth surface, came to be broken down at comparatively low applied load, i. e. nearly 10kg/cm^2 , may be recognized in the fact as shown in Fig. 14 and the following matter; we found minute substances as shown in Fig. 15 around the inner contact surfaces when the specimen was

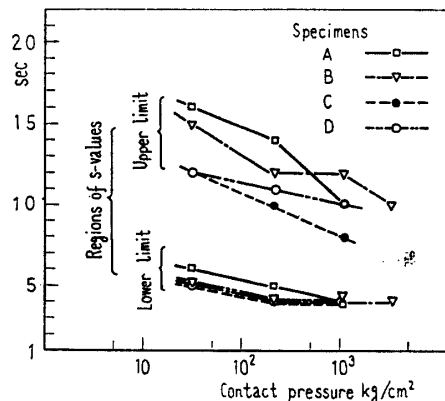


Fig. 13 Variation of distribution of s -values depending on contact pressure on nominal contact area

separated from the base plate.

The items of the minute substances were lapping powder and the broken bits of the surface irregularities, and the former may be considered some of the lapping powder which was separated from the specimen when the latter was deformed by the applied load, where the lapping powder

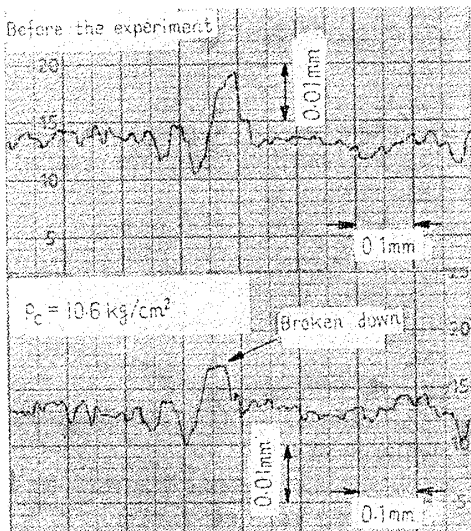


Fig. 14 An example of broken bit of surface irregularities

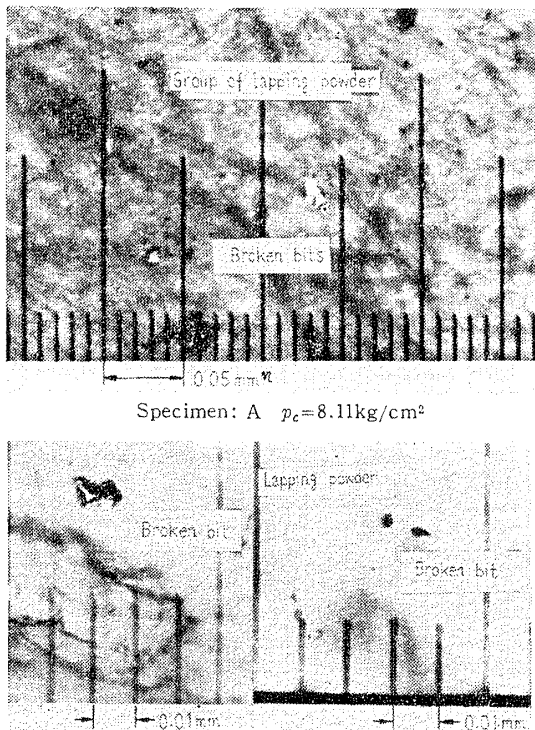


Fig. 15 Microphotograph of broken bits of surface irregularities and lapping powder separated from specimen

had been buried in the surface layer of specimen. These substances were found in steadily decreasing volumes with the progress of experiments, and occurred still at a high applied load, i. e. $p_{1c} \cong 32 \text{ kg/mm}^2$.

5.2.2 Central height of surface irregularities, h_c

It is as difficult to find the h_c -values under applied load as to do the s -values. The relations derived by the surface roughness under applied load are shown in Fig. 16.

It may be observed in the results of ex-

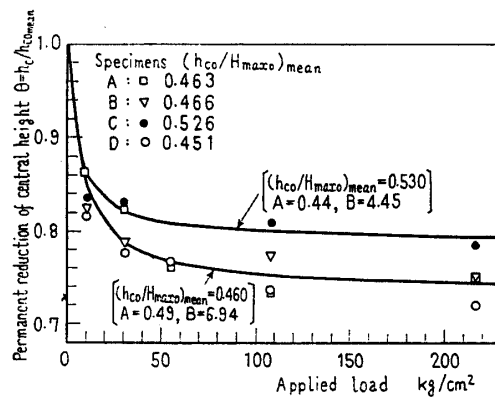
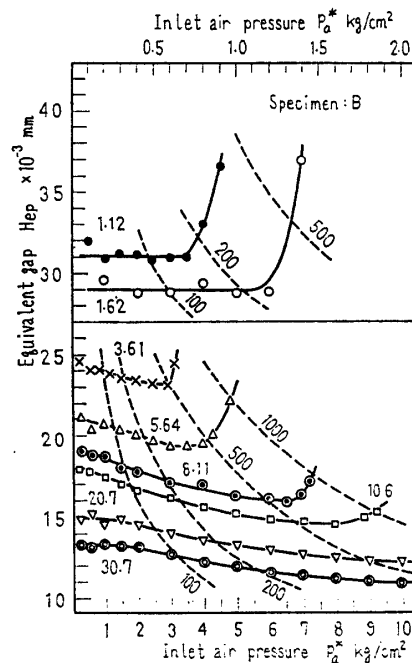


Fig. 16 Variation of central height of surface roughness depending on applied load

$$\theta = 1 - \{1 - (h_{c0}/H_{max0})_{mean}\} A e^{-B/\rho c}$$



Note: (1) Numerical values on full line are applied load in kg/cm^2
 (2) Numerical values on broken line are Reynolds number

Fig. 17 Relations between inlet air pressure and equivalent gap obtained by experimental results

periments that the values of the permanent reduction of central height tended so downward that the n -values became small, and then the experimental expression may be derived as follows:

$$\theta = \frac{h_c}{h_{c0\text{mean}}} = 1 - (1 - \eta)A \exp(-B/p_c) \dots \dots \dots (13)$$

where

$$\begin{aligned} \eta > 0.5 : A = 0.44, B = 4.45 \\ \eta < 0.5 : A = 0.49, B = 6.94 \end{aligned}$$

Introducing Eq. (13) into Eq. (11), therefore, the equivalent gap considering the variation of the h_c -values is given by

$$H_{ep} = \left[1.994 f_{(s)} \sqrt{\ln \left[1.117 \left(\frac{\sqrt{s}-1}{\sqrt{s}} \right)^2 \frac{k\sigma_s}{p_c} \left\{ \frac{k\sigma_s}{E} \left(\frac{\sqrt{s}-1}{\sqrt{s}} \right)^2 \right\}^{1-\alpha} \right]} - 1 \right] \theta_{hc0\text{mean}} \dots \dots \dots (14)$$

5.3 Equivalent gap between contact surfaces, H_{ep}

Assuming that the equivalent gap between contact surfaces is parallel clearance, Reynolds number at the inner outlet position of contact surfaces becomes equal to nearly 540 when the total flow rate of air-leakage is about $10^4 \text{ cm}^3/\text{min}$, and so the turbulent flow may occur in the beginning of the experiments of high inlet air pressure for every applied load, and in the other experiments it may be considered a viscous flow containing the region of the arising limit of turbulent flow⁽²⁾.

The H_{ep} -values in a certain range of experiments, accordingly, must be calculated as turbulent flow for them, but here the relations between inlet air pressure and the H_{ep} -values calculated by Eq. (25) of the 1st report assumed to be a viscous steady flow are shown in Fig. 17.

5.3.1 Variation of H_{ep} -values depending on inlet air pressure

The H_{ep} -values do not seem to vary at less than $p_a^* \cong 1 \text{ kg/cm}^2$ with no regard to the difference of surface roughness with or without applied load and the degree of the magnitude of applied load, but they seem to decrease as the inlet air pressure exceeds about 1 kg/cm^2 regardless of steady flow, and the reason for this may be considered the result of the sealing effect due to the minute substances in the space between contact surfaces.

5.3.2 Variation of H_{ep} -values depending on applied load

The relations between applied load and the H_{ep} -values given by about $p_a^* \cong 1 \text{ kg/cm}^2$ are shown in Fig. 18 in which are added the calculated curves given by Eq. (14). The calculated values obtained by assuming the surface irregularities as elasto-plastic were in agreement with the experimental values with a deviation within about 15%. The H_{ep} -values derived by introducing Eq. (13) into Eq. (23) of the 1st report, furthermore, were in good agreement with the results described above.

According to the results above-mentioned, it

may be considered that the H_{ep} -values can be derived from the condition in which the deformation of surface irregularities was plasticity in place of elastoplasticity, for the specimens in the region of experiments, i. e. $p_c \leq 30 \text{ kg/cm}^2$.

5.4 Elastic behavior rate, κ

Introducing the H_{ep} -values, of which the relations obtained by Fig. 12 are shown in Fig. 19, into Eq. (26) in the 1st report, the values of elastic behavior rate are shown in Fig. 20; where the applied load of standard was 1.62 kg/cm^2 .

The values have a tendency to diminish when the applied load is 10 kg/cm^2 and to increase with an increase in the applied load.

The κ -values calculated under each of the

Table 7 Elastic behavior rate with low applied loads after some increased applied loads

Increased applied loads p_{c1} kg/cm ²	Elastic behavior rate κ % (Applied load of standard $p_c = 1.62 \text{ kg/cm}^2$)							
	5.64 kg/cm ²				10.6 kg/cm ²			
	Specimens				Specimens			
	A	B	C	D	A	B	C	D
2.16×10^2	—	—	—	~100	—	—	~100	~100
5.40×10^2	~100	~100	—	~100	—	—	—	—
1.08×10^3	—	—	—	—	64	73	88	92
3.24×10^3	—	—	—	—	~100	~100	—	—

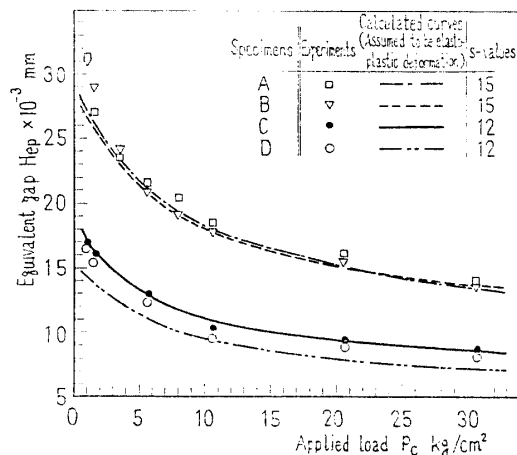


Fig. 18 Relations between applied load and equivalent gap

increased applied loads, furthermore, are listed in Table 7. It seems that the deformation of surface irregularities tends to be elastic gradually under a low applied load subsequent to an increased load.

5.5 Balance condition between contact surfaces

It is probable that the sudden increase of air-

leakage as shown in Fig. 11 will be caused by a push up of the specimen as the result of the supplied air pressure between contact surfaces becoming higher than the applied load. The physical meaning of the above may be considered as follows. The fluid pressure at any point on contact surface will be given in the 1st report as follows :

$$p^2 = p_a^2 - (p_a^2 - p_i^2)(\ln r_{0r} / \ln r_{0i}) \dots\dots\dots(15)$$

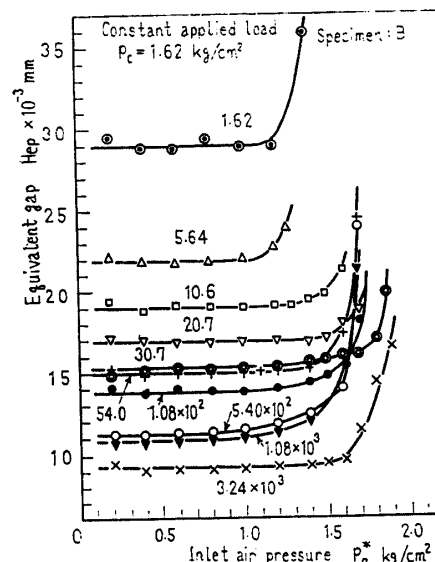
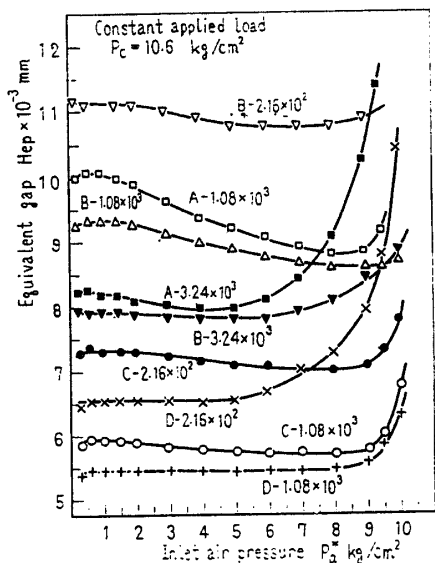
Here, the positive sign should be adopted only for the fluid pressure, and then

$$p = p_a \sqrt{1 - a \ln r_0} \sqrt{1 + b \ln r} \dots\dots\dots(16)$$

where

$$\left. \begin{aligned} a &= (1 - p_{ia}^2) / \ln r_{0i} \\ b &= a / (1 - a \ln r_0) \end{aligned} \right\} \dots\dots\dots(17)$$

$p_{ia} = p_i / p_a$
The total fluid pressure which separates the



- Note: (1) The meaning of symbols of A, B, C and D is shown in Table 4
 (2) The numerical values are the applied loads in kg/cm^2
 (3) The values of constant applied load should be replaced 1.62 kg/cm^2 with 1.68 kg/cm^2 for the experimental curves of 20.7 and 30.7 kg/cm^2

Fig. 19 Relations between inlet air pressure and equivalent gap obtained by experimental results shown in Fig. 12

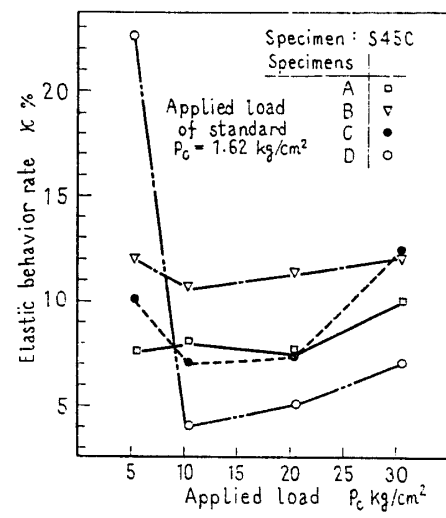


Fig. 20 Relations between applied load and elastic behavior rate

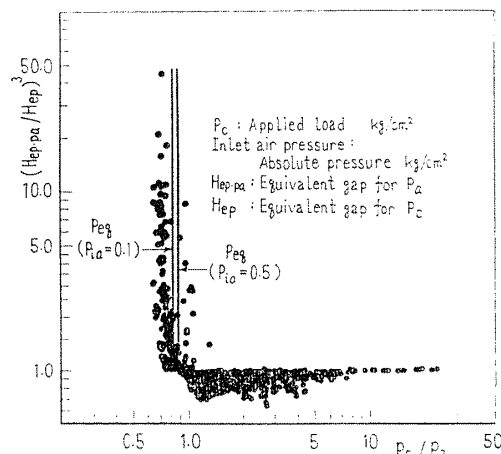


Fig. 21 Balance conditions between applied load and inlet air pressure

specimen from contact surface, accordingly, will be given by

$$P = \int_{r_i}^{r_o} 2\pi r p dr = \sqrt{\frac{a}{2}} \pi p_a e^{-2/b} \left[\sum_{n=0}^{\infty} \frac{1}{n!} \frac{2}{(2n+3)} t^{n+\frac{3}{2}} \right]_{t=2(1+b \ln r_i)/b}^{t=2(1+b \ln r_o)/b} \dots\dots\dots(18)$$

where

$$|t| < \infty$$

Here, the balance condition between applied load and supplied gas pressure between contact surfaces will be given by

$$P = p_c S_n \dots\dots\dots(19)$$

Introducing Eqs. (17) and (18) into Eq. (19), consequently, the balance condition will be derived as follows :

$$p_{eq} \equiv (p_c/p_a)_{eq} = \sqrt{\frac{a}{2}} \pi \frac{e^{-2/b}}{S_n} \left[\sum_{n=0}^{\infty} \frac{1}{n!} \frac{2}{(2n+3)} t^{n+\frac{3}{2}} \right]_{t=2(1+b \ln r_i)/b}^{t=2(1+b \ln r_o)/b} \dots\dots\dots(20)$$

The characteristics derived from the experimental values in the region of $R_e < 200$ are shown in Fig. 21.

The values of p_{eq} will be varied with the values of p_{ia} , and then the p_{eq} -values will be about 0.87 and 0.83, respectively, for the conditions in which the p_{ia} -values are 0.5 and 0.1 for the dimension of specimen.

The values of p_c , furthermore, will be obtained as the sum of the spring force and the frictional force of O-ring; the values of the latter were 1.4~1.8kg in the experiments and the value of arithmetic mean, i. e. 1.6kg, was adopted for the experiments. The experimental values are considered to agree well with the analytical results.

6. Conclusions

Assuming that the surface irregularities had a form of similar truncated cone in the same manner as the 1st report and the deformation of the truncated cone was elasto-plastic, the analytical expressions of equivalent gap for the fluid leakage between contact surfaces were derived considering the permanent reduction of the central height of surface irregularities under applied load. The results of comparison with the experiments were as follows.

(1) The H_{ep} -values calculated by assuming the surface irregularities as elasto-plastic were in agreement with the experimental values with a deviation within about 15% in the region of $p_c \leq 30\text{kg/cm}^2$.

The values obtained by assuming the surface irregularities as ideally plastic, furthermore, were derived in the same results as above.

According to the results described above, it seems that the H_{ep} -values can be derived from the condition in which the deformation of surface irregularities is plasticity in place of elasto-plasticity for the specimens in the region of $p_c \leq 30\text{kg/cm}^2$.

(2) The analytical expression of the balance conditions between applied load and supplied gas pressure between contact surfaces was derived and the analytical results were found in good agreement with the experimental values.

(3) The values of elastic behavior rate have a tendency to drop at a comparatively low applied load, i. e. nearly 10kg/cm² for the specimens, and to increase with an increase in the applied load.

It seems that the deformation of surface irregularities tends to be elastic gradually at a low applied load subsequent to application of a certain load, i. e. 200kg/cm² or more for the specimens.

(4) It is recognized as the phenomenon that one part of the irregularities on the real contact surfaces of rough surface, of the specimen which was pressed against a rigid smooth surface, comes to be broken down at a comparatively low applied load and some part of lapping powder, which has been buried in the surface layer of specimen, is separated from the specimen. It is believed that these minute substances have an effect of sealing the space between contact surfaces.

Appendix

The terms of the square root in Eq. (3) will be expanded in an infinite series as follows ;

$$\sqrt{\dots} = 1 + 2(H-Z_0)(X/HY^2) - 2(H-Z_0)^2 \times (X/HY^2)^2 + 4(H-Z_0)^3(X/HY^2)^3 + \dots\dots$$

and if we retain terms up to fourth inclusive in the expansion of the square root, then the residue will be

$$R = -10 \left(\frac{X}{Y^2} \right)^4 \left(\frac{H-Z_0}{H} \right)^4 \times \left[\frac{1}{\{1 + 4\theta(H-Z_0)(X/HY^2)\}^{7/2}} \right]$$

where

$$0 < \theta < 1$$

and the terms in the square brackets will be necessarily smaller than unity and that of $\{(H-Z_0)/H\}^4$

will be under unity. Thus,

$$|R| < 10(X/Y^2)^4$$

Here, the values of residue will be illustrated by an example as follows; the material is S45C, $E=2.1 \times 10^4$ kg/mm², $\sigma_s=35$ kg/mm², $2\gamma=135^\circ$, $k=2.20$ and we take 10^2 for the s -values, and then $(X/Y^2) \doteq 1/33.7$ and $|R| < 10^{-5}$. Hence, it will be considered satisfactory for the applied load on any truncated cone that the terms of square root be retained up to 4th inclusive. According to the results above-mentioned, Eqs. (4.a) and (4.b) could be derived, and then we may consider Eq. (4.a) for the first time as follows.

Now, we put

$$\{(H-Z_0)/H\}(X/Y^2) = \varepsilon$$

and then

$$P_m = \{(Y/X)H\}^2 [1 + 2\varepsilon \{(1-\varepsilon)^2 + (3/2)\varepsilon\}]$$

where the 2nd terms in the square brackets will necessarily be a positive number, and so the expression will be described by

$$P_m > \{(Y/X)H\}^2$$

and if we take into account the numerical numbers in which are included $H=1 \times 10^{-3}$ mm, $h_c=0.5 \times 10^{-3}$ mm, $S_n=1$ mm² and $\beta=2.0$, then

$$P_m > 1.6 \text{ kg}$$

and, furthermore, the following will be obtained from Eqs. (11), (16) and (17) in the 1st report:

$$N = (2/3)(8/9\pi)^2 \{1 - (1/s\sqrt{s})\}^2 \\ \times S_n \varphi_{(s)} / h_c^2 \tan^2 \gamma \doteq 5.2 \times 10^3$$

Then the applied load on the nominal contact surface, i. e. $S_n=1$ mm², will be derived as follows.

$$\text{Applied load} = P_m \times N > 8.32 \times 10^3 \approx 10^4 \text{ kg}$$

and the value has no practical meaning.

According to the results above-mentioned, the applied load on any truncated cone will be given by Eq. (4.b).

References

- (1) Kazamaki, T., *Bull. JSME*, Vol. 12, No.53 (1969-10), p. 1011.
- (2) Research Association on Minute-leakage., *Jour. Japan Soc. Mech. Engrs.* (in Japanese), Vol. 68, No. 560 (1965-9), p. 1321.

Discussion

T. TSUKIZOE (Osaka University):

(1) I would like to ask the author about the reason for the deviations between the analytical and the experimental H_{ep} -values being magnified to as much as 15% in the 2nd report, whereas they were about 7% in the 1st report.

In the case in which the analytical expression of the 2nd report will be applied to the specimens that had been tested in the 1st report, I would like to know what will be the values of deviation.

(2) It seems that there is little difference in the characteristics between the plastic and the elasto-plastic deformations as shown in Figs. 4 in the 1st and the 2nd reports respectively.

I would like to ask, accordingly, about whether or not the elastic deformation of surface irregularities can be neglected.

(3) Assuming that the volume of surface irregularities on the upper side of average line has no variation in spite of the surface irregularities being deformed, the h_c -values must be independent of applied load.

I would like to know why the h_c -values diminished suddenly at a low applied load as shown in Fig. 16.

(4) The expression, i. e. $\xi_{p1} = \sqrt{P_m / \pi k \sigma_s} / \tan \gamma$ in Eq. (1), might mean $k \sigma_s = P_m / \{\pi (\xi_{p1} \tan \gamma)^2\}$, and then it can be supposed that the contact pressure on the actual contact area does

not change.

I would like to know about whether or not the expression is derived from the suggestion advanced as to the same origin with Reference (1) in the 1st report.

S. IWANAMI (Musashi Institute of Technology):

(5) I would like to ask about the meaning of Conclusion (2) and what expression is called the balance condition by author.

(6) I would like to have a more detailed explanation, furthermore, to know what is meant by the analytical values being in good agreement with the experimental results.

Author's closure

(1) We are grateful for the comments made and interest taken in this paper by professor T. Tsukizoe. Compared with the 1st report, the 2nd report shows that the deviation of H_{ep} -values between the analytical and the experimental results has come to increase in magnitude as pointed out, and the fact has resulted from the low applied loads such as the p_c -values being 1.12 and 1.62 kg/cm² with materials A, B and D as shown in Fig. 18. The reason is supposed to be that the analytical H_{ep} -values have increased in magnitude compared with the experimental H_{ep} -values at low applied loads, because the surface roughness has included abnormally high surface irregularities

which had no influence on the h_c -values, as shown in Fig. 7.

The analytical H_{ep} -values obtained by assuming the deformation of surface irregularities as elasto-plastic were in agreement with the experimental H_{ep} -values with a deviation within about 7%, which was the same as the results of the 1st report, in the case of both material C throughout the experiments and materials A, B and D with the applied loads above about 5kg/cm².

Next, in the case in which the analytical expression of the 2nd report is applied to the specimens which were tested in the 1st report, the deviation came to be magnified to about 7% in the same manner as the results of the 1st report.

The results above mentioned may stem from the fact that there was little difference between both Figs. 4 of the 1st and the 2nd reports, where the characteristics are shown.

(2) The deformation of the surface irregularities may be considered as fairly plastic at less than about $p_c=30\text{kg/cm}^2$ in both the specimens of the 1st and the 2nd reports. The investigations with both high applied loads and the other materials will be continued in future.

(3) The h_c -values may be independent of applied load as pointed out, assuming that the total volume of surface irregularities, in other words, the surface roughness in which abnormally high surface irregularities are included, does not change with an applied load, where the plastic deformation of the surface irregularities on actual contact area has no effects upon the h_c -values. The measurement of the real profiles of surface roughness may be difficult, depending on the difficulty of the records of completely identical places, the reproducibility of the profiles of the surface irregularities of steel and the degree of accuracy of instrument. The experimental results have been obtained as shown in Fig. 16 with the statistical investigation of the surface roughness collected by the present report.

According to the results mentioned above, the reason is not clear, and the investigation will have to be continued in future.

(4) The values of plastic deformation, i. e. ξ_{p1} are equivalent to the values derived in Reference (4) in the 1st report; to quote the words of References (4): "the limiting value of that force beyond which there begins a plastic flow of the material".

Thus, we agree to your opinion.

(5) We think that the analytical expression of balance conditions between applied load and

supplied gas pressure between contact surfaces has been derived from Eq. (20).

Assuming that the fluid pressure, that may be considered a phenomenon of leakage between contact surfaces due to the inlet fluid pressure when a thick cylinder is pressed against a rigid body having an ideal smooth surface, is a laminar inward flow with a parallel clearance, i. e. H_{ep} , and then it might be called the balance condition that the total fluid pressure, i. e. the values of Eq. (18), which separates the specimen from contact surfaces, has come to equal to the applied load, i. e. the terms of the right side of Eq. (19).

The balance condition will be influenced by the geometric form of specimen, the surface roughness of specimen, fluid pressure and applied load. It seems that the balance condition should take account of the elastic deformation^(*) of specimen in the case in which the more detailed relations might be required, and this will be investigated in future.

We are grateful for the comments and suggestions made on this paper by professor S. Iwanami, and especially, for one by which the confusion between the abscissa in Fig. 21, i. e. (p_c/p_a) , and the terms of left side of Eq. (20), i. e. $(p_c/p_a)_{eq}$, could be avoided.

(6) It seems that the specimen was pushed up as the result of the supplied air pressure between contact surfaces becoming higher than that given by Eq. (20) under the condition of applied load being provided.

Here, we consider the applied load as follows.

As a force to separate the specimen from the contact surfaces is generated by fluid pressure in the empty space between contact surfaces, the applied load has to be varied as the result, but the reduction of the applied load may be considered not to influence the equivalent gap, because the deformations of surface roughness are plastic, as described in the 1st report.

The relations mentioned above, accordingly, will be derived as follows:

$$\left[\frac{\text{The ratio of}}{\text{equivalent gap}} \right]^3 = \frac{\left[\frac{\text{Equivalent gap at any sup-}}{\text{plied air pressure, } H_{ep} p_a} \right]^3}{\left[\frac{\text{Equivalent gap at given}}{\text{applied load, } H_{ep}} \right]^3} \\ \propto (\text{The ratio of air flow rate}) \\ \text{versus } (p_c/p_a)$$

and then the above relations are shown in Fig. 21 in which every one of the applied loads is included.

It has been stated here that the analytical

(*) Nau B. S. and Turnbull, D.E., *1st Int. Conf. Fluid Sealing*, Paper D3, (1961-4), B.H.R.A.

values were in good agreement with the experimental values, from the results that a sudden increase quantities of air-leakage occurred very close to the values of p_{eq} .

It may be considered that the considerations described above, under which the fluid flow was assumed to be a laminar inward flow, should require some corrections depending on the elastic

deformation of specimen, the effect of anisotropy of surface roughness and the degree of the numerical values of surface irregularities, where the values of supplied air pressure become higher than that of the present report and the applied load become higher than the experimental values of the present report. These problems will be investigated in future.
